Effects of dielectric disorder on van der Waals interactions in slab geometries

David S. Dean,[1,2] Ron R. Horgan,[1,3] Ali Naji,[1,4,5,6] and Rudolf Podgornik[1,7,8,9]
[1]*Kavli Institute for Theoretical Physics, University of California, Santa Barbara, California 93106, USA*
[2]*Laboratoire de Physique Théorique, IRSAMC, Université Paul Sabatier, 118 Route de Narbonne, 31062 Toulouse Cedex 4, France*
[3]*DAMTP, CMS, University of Cambridge, Cambridge CB3 0WA, United Kingdom*
[4]*Department of Physics and Astronomy, University of Sheffield, Sheffield S3 7RH, United Kingdom*
[5]*Department of Physics, Department of Chemistry and Biochemistry, and Materials Research Laboratory, University of California, Santa Barbara, California 93106, USA*
[6]*School of Physics, Institute for Research in Fundamental Sciences (IPM), 19395-553 Tehran, Iran*
[7]*Department of Physics, Faculty of Mathematics and Physics, University of Ljubljana, SI-1000 Ljubljana, Slovenia*
[8]*Department of Theoretical Physics, J. Stefan Institute, SI-1000 Ljubljana, Slovenia*
[9]*Laborarory of Physical and Structural Biology, National Institutes of Health, Maryland 20892, USA*
(Received 17 July 2009; revised manuscript received 22 April 2010; published 13 May 2010)

We analyze the effects of disorder on the thermal Casimir interaction for the case of two semi-infinite planar slabs across an intervening homogeneous unstructured dielectric. The semi-infinite bounding layers are assumed to be composed of plane-parallel layers of random dielectric materials. We show that the effective thermal Casimir interaction at long distances is self-averaging and can be written in the same form as the one between nonrandom media but with the effective dielectric tensor of the corresponding random media. On the contrary, the behavior at short distances becomes random, and thus sample dependent, dominated by the local values of the dielectric constants proximal to each other across the central homogeneous unstructured dielectric layer. We extend these results to the regime of intermediate slab separations by using perturbation theory for weak disorder as well as by extensive numerical simulations for a number of systems where the dielectric function has a log-normal distribution. Numerical simulation completely corroborates all the main features of the disorder dependent thermal Casimir interaction deduced analytically.

DOI: 10.1103/PhysRevE.81.051117 PACS number(s): 05.40.−a, 03.70.+k, 03.50.De, 77.22.−d

I. INTRODUCTION

Among the different forces acting between macromolecular surfaces the Casimir (zero temperature and ideally polarizable surfaces) and van der Waals (finite temperature and nonideally polarizable surfaces) interactions are certainly the most ubiquitous and have thus been studied in exhaustive detail [1]. The van der Waals forces are particularly important in condensed soft and hard matter and present one of the two fundamental interactions in colloid science [2]. In systems with spatially inhomogeneous dielectric properties the van der Waals forces arise from the fluctuation—thermal as well as quantum—driven interaction between transient and/or fixed dipoles within the interacting media [3]. Within the celebrated Lifshitz theory of van der Waals interactions [4,5] the thermal contribution to these fluctuation interactions is described by the zero frequency response of the dielectric function whereas the quantum component to the fluctuation interactions is given by the sum over the Matsubara frequencies of the dielectric response functions of the interacting media. Since the van der Waals interactions thus depend on the full dielectric dispersion spectra of the media involved they are also referred to as the dispersion interactions. Though there are obviously clear physical differences underlying the classical and the quantum contributions to the full van der Waals force, the computation of the corresponding interaction free energies is almost identical and can be formulated in terms of an appropriate functional determinant for the fluctuating electromagnetic field in a geometry particular to the interaction problem at hand. For the interaction between two homogeneous semi-infinite dielectric half-spaces across a finite dielectric slab the full Lifshitz theory of van der Waals—dispersion interactions [5] is thus based on appropriate boundary conditions imposed on the electromagnetic field at the bounding surfaces of the slab as well as the fluctuation-dissipation theorem that converts the fluctuating electromagnetic potential operators into corresponding dielectric response functions. From the full Lifshitz formulation one can derive the original Casimir interaction [6] by taking the limit of zero temperature and ideally polarizable bounding surfaces. In this respect the Lifshitz theory is then nothing else but a proper finite temperature and realistic boundary conditions generalization of the Casimir interaction [4]. The Lifshitz–van der Waals interactions are thus just the thermal Casimir effect.

Among the major mathematical problems in the computation of Casimir type interactions (setting aside the experimental and theoretical challenges to determine the correct dielectric behavior [1]) are the following:

(i) the application of the Lifshitz approach to nontrivial geometries (i.e., beyond the cases of planar, spherical and cylindrical geometries) and

(ii) taking into account local inhomogeneities in the dielectric properties of the media, always present in realistic systems and thus relevant for the comparison of theory with experiment.

In this paper, we will address the second of these points in detail and consider the effects of disorder in the composition of the bounding semi-infinite layers on the van der Waals interaction between them. To our knowledge we present the first analysis of the effect of dielectric disorder on Lifshitz–

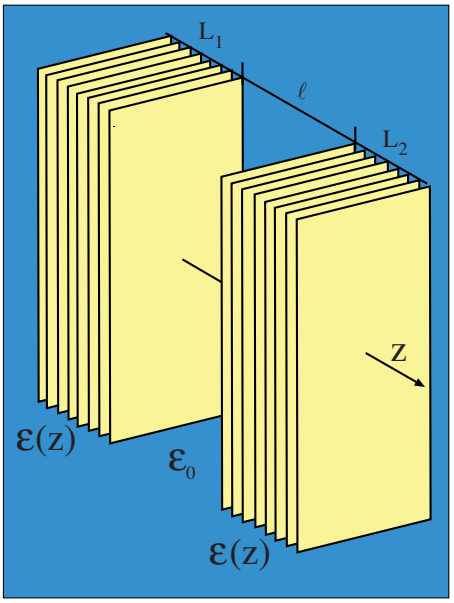

FIG. 1. (Color online) A schematic presentation of the model. Two finite slabs with disordered plane-parallel dielectric layers interacting across a dielectrically homogeneous slab of thickness ℓ. z axis is perpendicular to the plane of the slabs.

van der Waals interactions (apart from a recent letter [7] by the authors on this subject). Let us add that recently the effect of charge disorder on interactions between planar slabs has been analyzed in [8] where it was shown that, even if the slabs are net neutral, the presence of frozen charge disorder could drastically modify the long-range interslab interaction.

Specifically, we will consider the thermal (zero frequency) Casimir interaction for the case where the local dielectric constant in the bounding layers is a random variable described within a certain model of the disorder. We will evaluate the interaction between two semi-infinite planar dielectric slabs with dielectric disorder, separated by a homogeneous dielectric medium, see Fig. 1. In the model description of the disorder in the dielectric response that we consider here we will assume that the dielectric response function is constant within the two slabs in the planes perpendicular to the slab normal, but varies in the direction of the surface normal. It is well known that the simpler problem without any disorder where the dielectric constants of the slabs do not vary and are strictly homogeneous can be solved explicitly [4]. One could in principle tentatively apply this straightforward result of the Lifshitz theory to the case of disordered dielectric constants via an effective medium theory which consists of replacing the fluctuating dielectric constant by an effective (spatially homogeneous within each of the slabs) dielectric tensor. Naively one might try the approximation

$$\epsilon(\mathbf{x}) \to \langle \epsilon \rangle, \tag{1}$$

where the angular brackets denote the spatial or ensemble averaged dielectric constant within the slab in question. However in the most commonly used approximation the local dielectric tensor is simply replaced by an effective dielectric tensor [3,4], i.e.,

$$\epsilon_{ij}(\mathbf{x}) \to \epsilon_{ij}^{(e)}, \tag{2}$$

where the bulk dielectric tensor is defined via

$$\epsilon_{ij}^{(e)} \langle E_j \rangle = \langle \epsilon_{ij} E_j \rangle. \tag{3}$$

The use of the effective dielectric tensor is not universal and is not always easily justifiable mathematically as an approximation, although physically it clearly does capture the bulk response to constant electric fields. We shall see in this paper, for the random layered dielectric model studied here, that the effective dielectric constant approximation of Eq. (2) does in fact give the correct value of the thermal Casimir interaction in the limit where the two slabs are separated by a wide gap.

One can argue that this is to be expected on physical grounds as the fluctuating electromagnetic field modes with small wave vector (corresponding to variations on large scales) dominate the Casimir interaction for large intersurface separations. The dielectric response of the material to a constant electric field in that case is given by the effective dielectric constant and if the wave vector dependent response is suitably analytic near $\mathbf{k}=0$ we expect that $\epsilon_{ij}^{(e)}(\mathbf{k}) \sim \epsilon_{ij}^{(e)}(0) = \epsilon_{ij}^{(e)}$ for $|\mathbf{k}| \ll 1$.

It is much more difficult to come up with similar intuitively clear or at least plausible arguments as to what might happen to thermal Casimir interactions between disordered bounding layers in the opposite limit of small separations and/or for the separations in between the two limits. As we will demonstrate in what follows by applying a properly formulated perturbation theory and numerically solved models of disorder based on the random telegraph model and a log-normal distribution of the dielectric function, the fluctuation interaction in the limit of small separations becomes sample specific and is dominated by the local values of the dielectric constants of regions that are proximal to each other across the central homogeneous dielectric slab.

II. MODEL AND GENERAL ANALYSIS

A. Formulation

The Hamiltonian associated with the thermal fluctuations of the electrostatic field in a dielectric medium is given by the classical electromagnetic field energy

$$H(\phi) = \frac{1}{2} \int d\mathbf{x} \epsilon(\mathbf{x}) [\nabla \phi(\mathbf{x})]^2, \tag{4}$$

and the corresponding partition function is given by the functional integral

$$Z = \int d[\phi] \exp(-\beta H[\phi]). \tag{5}$$

Differences in dielectric constants lead to the thermal Casimir effect which arises from the full treatment of the thermal (zero frequency) van de Waals forces in the system. Here we will consider layered systems where the dielectric con-

stant ϵ only depends on the z direction $\epsilon(\mathbf{x})=\epsilon(z)$. If we express the field ϕ in terms of its Fourier modes in the plane perpendicular to z, coordinates denoted by $\mathbf{x}_\perp$ and which we will take to be of area A, with wave vector $\mathbf{k}=(k_x,k_y)$ then the Hamiltonian can be written as

$$H=\sum_{\mathbf{k}} H_{\mathbf{k}}, \tag{6}$$

with

$$H_{\mathbf{k}}=\frac{1}{2}\int dz\epsilon(z)\left(\frac{d\tilde{\phi}(z,\mathbf{k})}{dz}\frac{d\tilde{\phi}(z,-\mathbf{k})}{dz}+\mathbf{k}^2\tilde{\phi}(z,\mathbf{k})\tilde{\phi}(z,-\mathbf{k})\right). \tag{7}$$

A direct consequence of this decomposition of the Hamiltonian is that the partition function can be expressed as a sum over the partition function of the individual modes $Z_{\mathbf{k}}$ as

$$\ln(Z)=\sum_{\mathbf{k}}\ln(Z_{\mathbf{k}}), \tag{8}$$

where

$$Z_{\mathbf{k}}=\int d[X]\exp\left(-\frac{1}{2}\int dz\epsilon(z)\left[\left(\frac{dX}{dz}\right)^2+k^2X^2\right]\right), \tag{9}$$

where $k=|\mathbf{k}|$. In the above we have taken into account that the field ϕ is real and absorbed the common prefactor β into the variable X.

B. Evaluation of the functional integral

The problem of computing the interaction between slabs composed of layers of finite thickness can be studied using a transfer-matrix method [9]. However we will use a method based on the Feynman path integral instead, which is particularly well suited to the study of systems where the dielectric constant can vary continuously in only one direction [10]. If we specify the starting and finishing points of the above path integral to be x and y, respectively, at *times* z' and z we see that it has to be of harmonic oscillator form defined by

$$K(x,y;z',z)=\int_{X(z')=x}^{X(z)=y} d[X]\times\exp\left(-\frac{1}{2}\int_0^z dzM(z)\left[\left(\frac{dX}{dz}\right)^2+\omega^2X^2\right]\right), \tag{10}$$

where the mass, which is z dependent, is given by $M(z)=\epsilon(z)$ and the frequency ω is given by $\omega=k$. In the case where M and ω are constant, the propagator K is given by the well known formula

$$K(x,y;z',z,M,\omega)=\left\{\frac{M\omega}{2\pi\sinh[\omega(z-z')]}\right\}^{1/2}\times\exp\left[-\frac{1}{2}\{(x^2+y^2)M\omega\coth[\omega(z-z')]-2xyM\omega\,\mathrm{cosech}[\omega(z-z')]\}\right] \tag{11}$$

In the case where M (or indeed ω) vary with z we can still formally compute the path integral via the generalized Pauli–van Vleck formula which tells us that K must have the general form

$$K(x,y;z',z)=\left(\frac{b}{2\pi}\right)^{1/2}\exp\left(-\frac{1}{2}a_i(z',z)x^2-\frac{1}{2}a_f(z',z)y^2+b(z',z)xy\right). \tag{12}$$

We may now write down an evolution equation for the coefficients a_i, a_f, and b using the Markov property of the path integral (in fact this is how one can prove the generalized Pauli–van Vleck formula [10])

$$K(x,y;z',z+\zeta)=\int dwK(x,w;z',z)K(w,y;z,z+\zeta). \tag{13}$$

Now if we take $\zeta=\Delta z$ infinitesimal and assume that M and ω are constant over $(z,z+\Delta z)$ (but could have jumped at z), then by looking at the coefficients of x^2, y^2, and xy in $K(x,y;z+\Delta z)$, Calculated from Eq. (13) we find the following evolution equations for a_i, a_f, and b:

$$\frac{\partial a_i(z',z)}{\partial z}=-\frac{b^2(z',z)}{M}, \tag{14}$$

$$\frac{\partial b(z',z)}{\partial z}=-\frac{b(z',z)a_f(z',z)}{M}, \tag{15}$$

$$\frac{\partial a_f(z',z)}{\partial z}=M(z)\omega^2(z)-\frac{a_f^2(z',z)}{M(z)}. \tag{16}$$

Note that the evolution equation for b can also be obtained by examining the change in the pre-factor term of the propagator K. As the action is positive definite we expect that both a_i and a_f are positive (by considering paths starting or ending at 0). Also for $|z-z'|$ large, with respect to the correlation length of the disorder, we expect K to factorize in its x and y dependence and thus the coefficient b should decay to zero for sufficiently thick slabs. Note that if ϵ is a stationary process then the path integral should be the same run backward in time, z, as when it is run forward. This means that a_i and a_f should have the same steady state distribution.

Consider a system of two thick slabs of respective thicknesses L_1 and L_2 separated by a distance l and the region between them occupied by a dielectric medium of dielectric constant ϵ_0—vacuum or air, for example. From our discussion above, for large L_1 and L_2 the partition function for the mode $\mathbf{k}$ is thus proportional to

$$Z_{\mathbf{k}}=\int dxdy\exp\left[-\frac{1}{2}a_f^{(1)}(k)x^2\right]\left[\frac{\epsilon_0 k}{2\pi\sinh(kz)}\right]^{1/2}\times\exp\left\{-\frac{1}{2}[(x^2+y^2)\epsilon_0 k\coth(kz)-2xy\epsilon_0 k\,\mathrm{cosech}(kz)]\right\}\times\exp\left[-\frac{1}{2}a_f^{(2)}(k)y^2\right], \tag{17}$$

where $a_f^{(1)}(k)$ is the solution of Eq. (16) with some initial conditions (which for an infinite slab do not have to be specified) given at $z=z'=-L_1$ to zero with $\omega=k$ and $M(z)=\epsilon(z)$ and $a_f^{(2)}(k)$ is the corresponding quantity for the slab 2 (with initial conditions given at $z=z'=L_2+l$ and evaluated at $z=l$).

We thus find that the l-dependent part of the free energy of the mode $\mathbf{k}$ (up to a bulk term which can be subtracted off to get the effective interaction.) is given by

$$F_{\mathbf{k}} = \frac{k_B T}{2} \ln\left(1 - \frac{(a_f^{(1)}(k)-\epsilon_0 k)(a_f^{(2)}(k)-\epsilon_0 k)}{(a_f^{(1)}(k)+\epsilon_0 k)(a_f^{(2)}(k)+\epsilon_0 k)} \exp(-2kl)\right), \tag{18}$$

with the total l dependent free energy given by

$$F = \sum_{\mathbf{k}} F_{\mathbf{k}}. \tag{19}$$

In order to evaluate the integrals of $a_f^{(1,2)}(k)$, one first has to solve equations of motion Eqs. (16) to get the z dependence of $a_f(k,z)$ and then proceed to the integrals that enter Eq. (18). The evolution equation for $a_f(k)$ for either slab can be read of from Eq. (16) and is given by

$$\frac{da_f(k,z)}{dz} = \epsilon(z)k^2 - \frac{a_f^2}{\epsilon(z)}, \tag{20}$$

where we have dropped the explicit dependence on the initial point $z'=-L_1$. Though it does not look like it at first sight, this equation is simply a rewriting of the underlying Poisson equation for the original, charge free, dielectric system. This can be seen as follows. Assume first of all that $a_f(k,z)$ can be parameterized with a function $\Psi(k,z)$ as

$$a_f(k,z) = \epsilon(z)\frac{d}{dz}\ln \Psi(k,z). \tag{21}$$

In quantum mechanics problems with disorder the above change of variables is often used since in the presence of disorder the nonlinear first order equation is easier to analyze then the second order linear equation [11]. Inserting now this *ansatz* back into Eq. (20) we find that it implies

$$\frac{d}{dz}\left(\epsilon\frac{d\Psi}{dz}\right) - \epsilon k^2 \Psi = 0 \tag{22}$$

for $\Psi(k,z)$, which is nothing but the Poisson equation for an inhomogeneous dielectric, where the inhomogeneity is only in the z direction and which has been Fourier transformed in the directions perpendicular to z. The function $a_f(k,z)$ in Eq. (21) is thus given by the solution of the Poisson equation in the specified planar geometry. This is of course no surprise since we are indeed dealing with an inhomogeneous electrostatic problem. On the other hand the derivation presented above is completely equivalent to the transfer matrix method [9] or to the density functional method [12] for evaluating the van der Waals forces. One of the clear strengths of this method is that it allows the of computation the van der Waals interaction to be carried out using a local method where the coefficients a_f, a_f, and b for any of the media involved can be computed and then the interactions between any combinations of media can be worked out in terms of these coefficients.

If we now write $a_f^{(i)}(k,z)=k\alpha^{(i)}(k,z)$ and if the distributions of the $\alpha^{(i)}(k,z)=y$ are given by $p_i(k,y)$ then we find that, in three dimensions the average l dependent free-energy is given by

$$\langle F\rangle = \frac{k_B T A}{4\pi}\int dk k \int dy_1 \int dy_2 p_1(k,y_1)p_2(k,y_2) \times \ln\left(1 - \frac{(y_1-\epsilon_0)(y_2-\epsilon_0)}{(y_1+\epsilon_0)(y_2+\epsilon_0)}\exp(-2kl)\right), \tag{23}$$

where the angular brackets on the left-hand side indicate the disorder average over the dielectric constant within the slabs and we have assumed that the realizations of the disorder in the two slabs are independent. This is why the joint disorder probability distribution is multiplicative for the two layers.

In the case where the slab thickness is large, $L\to\infty$, it is simple to derive a scaling formula from Eq. (20) for the probability distribution. Let $\epsilon(z)=\epsilon_g f(z)$ where $f(z)$ is an instance drawn from an ensemble distributed according to a given distribution. Then $p(k,y;\epsilon_g)$ is the resulting distribution for y given the mode wave-vector k. We then find that

$$p(k,y;\lambda\epsilon_g) = \frac{1}{\lambda}p(k,y/\lambda;\epsilon_g). \tag{24}$$

Thus, we need to compute the probability distribution once only, say, for $\epsilon_g=1$, and obtain those for other values of ϵ_g using this scaling result.

C. Large l limit

Let us first investigate the form of the van der Waals interaction free energy in the limit of large separations between the two slabs. The equation obeyed by α is

$$\frac{d\alpha(k,z)}{dz} = \epsilon k - \frac{k\alpha^2}{\epsilon}, \tag{25}$$

which can be written as

$$\frac{d\alpha(k,\zeta)}{d\zeta} = \epsilon(\zeta/k) - \frac{\alpha^2}{\epsilon(\zeta/k)}, \tag{26}$$

with $\zeta=zk$. When k is small $\epsilon(\zeta/k)$ varies very rapidly and thus becomes de-correlated from the value of α. The Laplace transform for the probability density function of α is defined by

$$\tilde{p}(k,s,\zeta) = \int_0^\infty dy\, \exp(-sy)p(k,y,\zeta) = \langle \exp[-s\alpha(k,\zeta)]\rangle, \tag{27}$$

and, from the equation of motion Eq. (25), obeys

$$-\frac{1}{s}\frac{d\tilde{p}(k,s,\zeta)}{d\zeta} = -\frac{1}{s}\frac{d}{d\zeta}\langle \exp[-s\alpha(k,\zeta)]\rangle$$
$$= \left\langle \epsilon(\zeta/k)\exp[-s\alpha(k,\zeta)] - \frac{\alpha^2}{\epsilon(\zeta/k)}\exp[-s\alpha(k,\zeta)]\right\rangle. \quad (28)$$

Assuming that k is small and thus $\alpha(k,\zeta)$ and $\epsilon(\zeta/k)$ are decorrelated we can write

$$-\frac{1}{s}\frac{d\tilde{p}(k,s,\zeta)}{d\zeta} = \langle\epsilon\rangle\tilde{p}(k,s,\zeta) - \langle 1/\epsilon\rangle\frac{d^2}{ds^2}\tilde{p}(k,s,\zeta). \quad (29)$$

This equation has the large ζ equilibrium solution (justified as we are taking the limit $L_1, L_2 \to \infty$)

$$\lim_{\zeta\to\infty}\tilde{p}(k,s,\zeta) = \exp(-\epsilon^* s), \quad (30)$$

with

$$\epsilon^* = \sqrt{\frac{\langle\epsilon\rangle}{\langle 1/\epsilon\rangle}}. \quad (31)$$

Inverting the Laplace transform then gives the equilibrium distribution

$$p(y,k) = \delta(y-\epsilon^*), \quad (32)$$

at small k. When l is large the integral in Eq. (23) is dominated by the small k behavior and we may use the analysis presented above, especially Eq. (32) in Eq. (23), to give the following asymptotic form for the interaction free energy

$$\langle F\rangle(l\to\infty) \sim \frac{k_B T A}{16\pi l^2}\int u du \ln[1-\Delta_1^*\Delta_2^*\exp(-u)] \sim -\frac{H^*}{l^2}, \quad (33)$$

with

$$\Delta_i^* = \frac{(\epsilon_i^* - \epsilon_0)}{(\epsilon_i^* + \epsilon_0)}, \quad (34)$$

and where ϵ_i^* are defined via Eq. (31). The subscript i on the angled brackets signifies that we are averaging the dielectric constant in the slab i. The term H^* defines an effective disorder-dependent Hamaker coefficient.

This rigorous result can be shown to coincide with that obtained from a more physical argument. We assume that the random layered material can be replaced by an effective anisotropic medium where the dielectric tensor is nonisotropic and must from symmetry considerations have the form

$$\epsilon_{zz}^{(e)} = \epsilon_{\|}, \quad (35)$$

$$\epsilon_{xx}^{(e)} = \epsilon_{yy}^{(e)} = \epsilon_{\perp}, \quad (36)$$

all other terms being zero by symmetry. In general the effective dielectric constant for random media is difficult to compute, few exact results exist and one must often resort to approximation schemes such as effective medium theories. However as the underlying geometry of the disorder is one dimensional, the effective dielectric tensor can be evaluated exactly. The term $\epsilon_{\|}$ is the dielectric constant in the z direction is given by

$$\epsilon_{\|}^{(e)} = \frac{1}{\langle 1/\epsilon\rangle}, \quad (37)$$

and the perpendicular component is simply given by

$$\epsilon_{\perp}^{(e)} = \langle\epsilon\rangle. \quad (38)$$

The forms of $\epsilon_{\|}^{(e)}$ and $\epsilon_{\perp}^{(e)}$ follow simply from the fact that in the perpendicular direction the dielectric constant is obtained by analogy to capacitors in series and in the parallel direction by analogy to capacitors in parallel arrangement [13]. These results can also be understood in terms of effective diffusion constants for diffusions where the local diffusivity is given by $\epsilon(\mathbf{x})$ [14].

It is a straightforward exercise to see that the effective value of ϵ^* for this system coincides with that of Eq. (31) above. This correspondence makes physical sense since the high wavelength or small k fluctuations of the electric field are responsible for the behavior of the Casimir interaction at large distances and the effective dielectric response at low (but nonzero k) must be close to that of the response to a constant field, i.e., described in terms of a dielectric constant. An interesting consequence of this result is that for large separations (where l is much greater than the correlation length of the dielectric disorder) the thermal Casimir interaction free energy is self averaging.

It is instructive to compare the result for the Casimir interaction at large separations for the case of a fluctuating dielectric constant with the case of a homogeneous medium, whose dielectric constant is the average of that in the fluctuating medium: $\epsilon_h = \langle\epsilon\rangle$ (the subscript h signifying that the medium is homogeneous). The homogeneous medium has a Hamaker constant

$$H_h = -\frac{k_B T}{16\pi}\int u du \ln[1-\Delta_h^2\exp(-u)], \quad (39)$$

with

$$\Delta_h = \frac{\langle\epsilon\rangle - \epsilon_0}{\langle\epsilon\rangle + \epsilon_0}, \quad (40)$$

when medium (1) has the same composition as medium (2). Jensen's inequality tells us that

$$\langle 1/\epsilon\rangle \geq \frac{1}{\langle\epsilon\rangle}, \quad (41)$$

since the function $f(x)=1/x$ is convex. Thus

$$\epsilon^* = \sqrt{\frac{\langle\epsilon\rangle}{\langle 1/\epsilon\rangle}} \leq \langle\epsilon\rangle. \quad (42)$$

Clearly the effective Hamaker constant is a monotonic function of Δ^2 and the interaction is always attractive. The difference in Δ^2 for the two systems is

$$\Delta^{*2} - \Delta_h^2 = 4\frac{\epsilon_0(\epsilon^* - \langle\epsilon\rangle)(\epsilon^*\langle\epsilon\rangle - \epsilon_0^2)}{(\langle\epsilon\rangle + \epsilon_0)^2(\epsilon^* + \epsilon_0)^2}. \quad (43)$$

Therefore, using Eq. (42), we find that if $\epsilon^*\langle\epsilon\rangle > \epsilon_0^2$ then $H_h > H^*$, and the interaction between the two homogeneous media is stronger than that between the two fluctuating media. This condition can be written as

$$\frac{\langle\epsilon\rangle^3}{\langle 1/\epsilon\rangle} > \epsilon_0^4, \tag{44}$$

and is always satisfied if $\langle 1/\epsilon\rangle^{-1} > \epsilon_0$. However it is always violated (the interaction between the homogeneous media is weaker than that between the random media) if $\langle\epsilon\rangle < \epsilon_0$. We thus see that, depending on the details of the distribution of the fluctuating dielectric response in the two slabs and the dielectric response of the medium in-\ between, the effective interaction at large interslab separations can be stronger or weaker than that for a uniform medium with a dielectric constant equal to the average value of that of the media in which it fluctuates.

D. Small l limit

When considering the small l limit we must bear in mind that quantum effects (i.e., nonzero Matsubara frequencies) will eventually dominate the interaction at very short distances. The cross over between the thermal and quantum regimes occurs at $l_c \sim hc\beta$ and the crossover between the self averaging regime for the $n=0$ Matsubara mode and that where one sees the effects of disorder is given by the correlation length of the disorder ξ. Therefore the short distance behavior discussed here is experimentally relevant in systems where $\xi \gg l_c$.

One would imagine that as the distance between the slabs is reduced the result will be increasingly dominated by the slab composition at the two opposite faces [4]. Indeed in the small l limit Eq. (23) is dominated by the large k behavior. The asymptotic behavior can be extracted if one assumes the *ansatz*

$$\alpha(k,z) = \sum_{n=0}^{\infty} \frac{\alpha_n(z)}{k^n}. \tag{45}$$

Substituting this into Eq. (25) gives the following chain of equations for $\alpha_n(z)$

$$\frac{1}{k}\sum_{n=0}^{\infty}\frac{1}{k^n}\frac{d\alpha_n(z)}{dz} = \epsilon(z) - \frac{1}{\epsilon(z)}\sum_{n,m=0}^{\infty}\frac{\alpha_n(z)\alpha_m(z)}{k^{m+n}}. \tag{46}$$

From here it is easy to see that to order $O(1)$ the leading asymptotic result of Eq. (51) is given by

$$\alpha_0(z) = \epsilon(z). \tag{47}$$

The equation for the corrections ($n \geq 1$) to this asymptotic limit is

$$\frac{d\alpha_{n-1}(z)}{dz} = -\frac{1}{\epsilon(z)}\sum_{m=0}^{n}\alpha_m(z)\alpha_{n-m}(z), \tag{48}$$

and the next two terms in the asymptotic expansion are given by

$$\alpha_1(z) = -\frac{1}{2}\frac{d\epsilon(z)}{dz}, \tag{49}$$

$$\alpha_2(z) = \frac{1}{4}\frac{d^2\epsilon(z)}{dz^2} - \frac{1}{8\epsilon(z)}\left(\frac{d\epsilon(z)}{dz}\right)^2. \tag{50}$$

It is straightforward to realize that these terms generate $O(1/l)$ corrections to the asymptotic result which are subdominant when l is large. Thus to the leading order

$$\alpha(k,z) \approx \alpha_0(z) = \epsilon(z), \tag{51}$$

and from here it follows straightforwardly that

$$\lim_{k\to\infty} p_i(y,k) = \rho_i(y), \tag{52}$$

where ρ_i is the probability density function of $\epsilon(z)$ in medium i. This result is easily understood from the physical discussion above. The average of the thermal Casimir interaction free energy Eq. (23) in the small separation limit is thus given by

$$\langle F\rangle(l\to 0) \sim \frac{k_B T}{16\pi l^2}\int udu \int d\epsilon_1 d\epsilon_2 \rho_1(\epsilon_1)\rho_2(\epsilon_2) \times \ln[1-\Delta_1\Delta_2\exp(-u)], \tag{53}$$

with

$$\Delta_i = \frac{\epsilon_i - \epsilon_0}{\epsilon_i - \epsilon_0}. \tag{54}$$

The forms of the thermal Casimir interaction free energy are thus given by Eqs. (33) and (53) in the small and large interslab separation limits, respectively. We have obtained the limiting behavior of the thermal Casimir effect in the limit of large separation between the slabs, where the free energy is given by self-averaging and the distributions of $\alpha(k,z)$ are strongly peaked, and in the limit of small separation, where the free energy is a random variable that has to be averaged over the probability density function of the dielectric constant in the media composing the two interacting slabs.

III. SMALL DISORDER LIMIT—PERTURBATION THEORY

The analysis presented above is valid for any type of disorder, irrespective of its properties. Here we also investigate a different approach that takes into account the disorder effects on a perturbative level, i.e., another way of approaching this problem analytically is to assume that the disorder is small. We assume in this case that the dielectric response can be written with an *ansatz* of the form

$$\epsilon(z) = \epsilon_g \exp[\lambda\psi(z)], \tag{55}$$

where λ is a scalar parametrizing the strength of disorder which will be used as the expansion parameter for perturbation theory. When $\lambda=0$ we have the disorder-free homogeneous system which is the starting point for the perturbation expansion (zeroth order). If the mean of the field of ψ is zero then ϵ_g is the geometric mean of the dielectric constant. We now assume that λ is small and write

$$\alpha(k,z) = \sum_{n=0}^{\infty} \lambda^n \alpha_n(k,z). \tag{56}$$

Substituting this into Eq. (25) and matching the powers of λ, we obtain the following equations for the first three terms in the perturbation expansion when z is large:

$$\alpha_0 = \epsilon_g, \tag{57}$$

$$\frac{d\alpha_1}{dz} = k(-2\alpha_1 + 2\epsilon_g \psi), \tag{58}$$

$$\frac{d\alpha_2}{dz} = k\left(-2\alpha_2 - \frac{\alpha_1^2}{\epsilon_g} + 2\alpha_1 \psi\right). \tag{59}$$

At large z we can solve the last two equations to obtain

$$\alpha_1 = 2k\epsilon_g \int_0^z dz' \exp[-2k(z-z')]\psi(z'), \tag{60}$$

$$\alpha_2 = 4k^2\epsilon_g \int_0^z dz' \exp[-2k(z-z')]\psi(z') \int_0^{z'} dz'' \times \exp[-2k(z'-z'')]\psi(z'') - 4k^3\epsilon_g \int_0^z dz \times \exp[-2k(z-z')]\left\{\int_0^{z'} dz'' \exp[-2k(z'-z'')]\psi(z'')\right\}^2. \tag{61}$$

We can now verify some of our previous results at the level of perturbation theory. For $k \to \infty$ we have that $2k \exp[-2k(z-z')] \to \delta(z-z')$, and this gives

$$\alpha_1 \to \epsilon_g \psi(z), \tag{62}$$

$$\alpha_2 \to \frac{\epsilon_g}{2}\psi^2(z). \tag{63}$$

This gives

$$\alpha \to \epsilon_g\left(1 + \lambda\psi + \frac{\lambda^2}{2}\psi^2\right) \approx \epsilon_g \exp(\lambda\psi) = \epsilon(z), \tag{64}$$

in agreement with the large k result stated previously. Also in the limit of small k we will have that

$$\lim_{k\to 0} 2k \int_0^z dz' \exp[-2k(z-z')]\psi(z') \to \langle\psi\rangle \tag{65}$$

for large z and so we have

$$\alpha_1 \to \epsilon_g \langle\psi\rangle, \tag{66}$$

$$\alpha_2 \to \frac{\epsilon_g}{2}\langle\psi\rangle^2. \tag{67}$$

Since $\langle\psi\rangle = 0$, we find

$$\lim_{k\to 0} \alpha(k,z) = \epsilon_g, \tag{68}$$

which is in agreement [to $O(\lambda^2)$] with the general result Eq. (31).

Now let us consider the case where the field ψ is Gaussian of zero mean with correlation function

$$\langle\psi(z)\psi(z')\rangle = \exp(-\omega|z-z'|), \tag{69}$$

where $1/\omega = \xi$ is the correlation length of the field (note that as, in the second order perturbation theory carried out here, the computation only involves the second moment of the field ψ the assumption of Gaussian statistics can be relaxed). This Gaussian field has the correlation function of an Orstein-Uhlenbeck (OU) process and is Markovian. The moments relevant to the degree in perturbation theory we are working to $[O(\lambda^2)]$ are

$$\langle\alpha_1\rangle = 0, \tag{70}$$

$$\langle\alpha_1^2\rangle = = \frac{2k\epsilon_g^2}{2k+\omega}, \tag{71}$$

$$\langle\alpha_2\rangle = \frac{k\epsilon_g}{2k+\omega}. \tag{72}$$

Using this we may write the corresponding free energy as a random variable

$$F = \frac{k_B T}{16\pi l^2} \int u du \ln[1 - \Delta_1'\Delta_2' \exp(-u)], \tag{73}$$

where

$$\Delta_i' = \frac{\epsilon_i' - \epsilon_0}{\epsilon_i' + \epsilon_0}, \tag{74}$$

with

$$\epsilon_i' = \epsilon_{g,i}\left(1 + \lambda\sqrt{\frac{u}{u+\omega_i l}}\sigma_i + \frac{\lambda^2}{2}\frac{u}{u+\omega_i l}\right). \tag{75}$$

The subscript i refers to the medium (1 or 2) and the σ_i are independent Gaussian random variables of zero mean and unit variance. Note that to order λ^2 we can replace the term α_2 by its mean and have done so in the above. Also we should expand the corresponding expression for the free energy to order λ^2, this will ensure that the resulting average and moments will always be finite.

IV. RANDOM TELEGRAPH SLAB MODEL

Here we will consider a model of dielectric disorder which we can solve exactly and which clearly demonstrates the general results about long distance and short distance behavior found in our previous analysis.

We consider a two composite model for the dielectric slabs. In a given slab we generate the random dielectric function by choosing one of two values ϵ_A or ϵ_B. The material keeps this same dielectric value for an exponentially distributed distance z of mean $1/\omega$. This means that the dielectric

constant switches between these two values with rate ω. The probability of observing either dielectric constant is thus equal and the distribution of the thickness of regions of the same dielectric constant has an exponential distribution. The random variable ϵ is Markovian and this fact allows us to write down an effective Fokker-Planck equation for the joint distribution of ϵ and the process α.

Let us denote by $p(A/B,y,z,k)dy$ the joint probability that the dielectric constant $\epsilon=\epsilon_{A/B}$ and that $\alpha\in[y,y+dy]$. Note that the distribution function for y is then given by the marginal distribution

$$p(y,z,k)=p(A,y,z,k)+p(B,y,z,k). \tag{76}$$

Using the equation of motion for α, Eq. (25), the evolution equation for $p(A,y,z,k)$ is derived by standard methods [15] to give

$$\frac{\partial}{\partial z}p(A,y,z,k)=-k\frac{\partial}{\partial y}[(\epsilon_A-y^2/\epsilon_A)p(A,y,z,k)]-\omega p(A,y,z,k)+\omega p(B,y,z,k), \tag{77}$$

together with the corresponding equation for $p(B,y,z,k)$. The equilibrium (large z) distributions are given by $p(A/B,y,k)$ which obey

$$k\frac{\partial}{\partial y}[(\epsilon_{A/B}-y^2/\epsilon_{A/B})p(A/B,y,z,k)]+\omega p(A/B,y,k)-\omega p(B/A,y,k)=0 \tag{78}$$

These probability density functions have a support over $y\in[\epsilon_A,\epsilon_b]$ where $\epsilon_A<\epsilon_B$ as from Eq. (25) we see that the process α, if started between the two extremal values ϵ_A and ϵ_B, stays between these two values. After some algebra we find the solutions

$$p(A,y,k)=\frac{C(k)\epsilon_A}{y^2-\epsilon_A^2}\left(\frac{(y-\epsilon_A)(\epsilon_B-y)}{(\epsilon_A+y)(\epsilon_B+y)}\right)^s, \tag{79}$$

$$p(B,y,k)=\frac{C(k)\epsilon_B}{\epsilon_B^2-y^2}\left(\frac{(y-\epsilon_A)(\epsilon_B-y)}{(\epsilon_A+y)(\epsilon_B+y)}\right)^s, \tag{80}$$

where the exponent $s=\omega/2k$. The constant $C(k)$ is determined from the normalization conditions $\int dy p(A/B,y,k)=1/2$.

This exact solution nicely demonstrates a number of the general features derived in Sec. II. For instance, we may write

$$p(A,y,k)=\frac{C(k)\epsilon_A}{y^2-\epsilon_A^2}\exp\left(-\frac{\omega}{2k}g(y)\right), \tag{81}$$

$$p(B,y,k)=\frac{C(k)\epsilon_A}{\epsilon_B^2-y^2}\exp\left(-\frac{\omega}{2k}g(y)\right), \tag{82}$$

where

$$g(y)=-\ln(y-\epsilon_A)-\ln(\epsilon_B-y)+\ln(\epsilon_A+y)+\ln(\epsilon_B+y). \tag{83}$$

We find that the minimum of $g(y)$ occurs at $y=\epsilon^*=\sqrt{\epsilon_A\epsilon_B}$. Thus as $k\to 0$ the distribution $p(y,k)$ becomes peaked around $y=\epsilon^*$. There also exists a critical value of $k=k^*$ with $k^*=\omega/2$ such that for $k<k^*$ we have $\lim_{y\to\epsilon_{A/B}}p(A/B,y,k)=0$, i.e., the density at the extremal values ϵ_A and ϵ_B is zero. However for $k>k^*$ we enter into a short distance regime where the density at ϵ_A and ϵ_B diverges and the extremal values are the most probable values. In the following section we will verify these predictions for the telegraph model numerically.

V. NUMERICAL SIMULATIONS

In this section, we present the results of numerical simulations of the models presented in earlier sections. We verify the general asymptotic behavior of the Casimir free energy that we have deduced, and compute the Hamaker variable, $H(l)$ (it is now generally a function of slab separation l), for various choices of parameters which determine the distribution of the local dielectric constant. We define $H(l)$ from the definition of the free energy $\langle F\rangle(l)$ given in Eq. (23) by

$$\langle F\rangle(l)=-\frac{H(l)}{l^2}. \tag{84}$$

To carry out the numerical study we first must construct the joint probability distributions $p_i(k,y)$ discussed in Sec. II B. This is done by choosing an instance of the field $\epsilon(z)$ from its defining distribution and then integrating Eq. (26) for a given value of k to obtain the large-z value of α: $\alpha(k,\zeta=\infty)$. We average over the ensemble by repeating this procedure many times and construct $p(k,y)$ by binning the results

$$p(k,y)\Delta y=\frac{n(y,\Delta y)}{N}, \tag{85}$$

where $n(y,\Delta y)$ is the number of values of $\alpha(k,\infty)$ lying in $[y,y+\Delta y]$ and N is the total number of evaluations. In our simulations we used $N=10^6-10^8$.

We first consider the telegraph model discussed in Sec. IV. The advantage of this model is that the evolution equations, Eqs. (26) and (77), can be solved exactly to give the asymptotic distributions $p(A/B,k,y)$ given in Eqs. (81) and (82). It was noted that there is a transition for $k=\omega/2$ where the distributions change from being zero at the extreme values $y=\epsilon_A$, $y=\epsilon_B$ for $k<\omega/2$, to diverging for for $k>\omega/2$. To verify the results numerically we choose $\omega=1$, $\epsilon_A=5$, $\epsilon_B=10$ and in Figs. 2 and 3 we show the results for $p(A,k,y)$ and $p(B,k,y)$, respectively, for values of k below and above the transition value. The continuous curves are the predicted functions from Eqs. (81) and (82), respectively. The normalization factors $C(k)$ was computed from a separate numerical integration. We see good agreement for both distributions $p(A/B,k,y)$ which thus verifies the analytic result. There is a minor discrepancy for $k=1.0$ which is a symptom of the discrete nature of the numerical procedure in

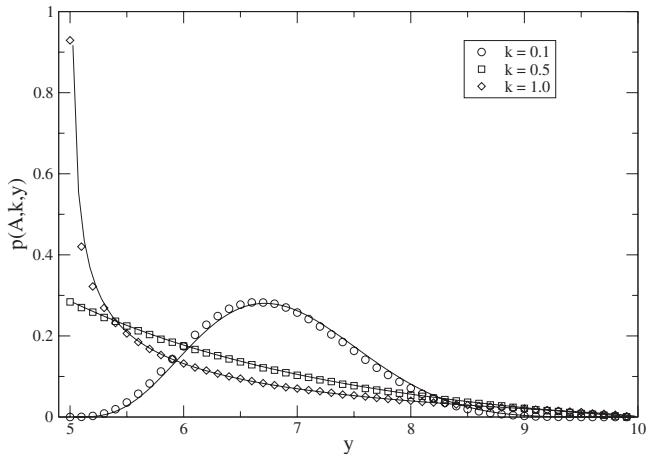

FIG. 2. Numerical and theoretical plots of the distribution $p(A,k,y)$ for the telegraph model defined in Sec. IV for $\epsilon_A=5.0$, $\epsilon_B=10.0$, $\omega=1.0$, and for $k=0.1,0.5,1.0$. The agreement is good and the minor discrepancy for $k=1.0$ is a symptom of the discrete nature of the numerical procedure. The value $k=0.5$ corresponds to the transition where $p(A,k,y)$ becomes nonzero at $y=\epsilon_A$. In general, for $k<1/2\omega$ we have $p(A,k,y=\epsilon_A)=0$ and for $k\geq 1/2\omega$ $p(A,k,y=\epsilon_A)>0$. This behavior has a strong effect on the Hamaker coefficient.

this case. We can see that the prediction that $p(A/B,k,y)$ peaks at the geometrical mean ($\sqrt{50}\sim 7.07$ here) in the large k limit is already evident.

To compute the Hamaker coefficient $H(l)$ for the telegraph model we use Eqs. (23) and (84) with the probability distribution given in Sec. IV, Eqs. (79) and (80). One difficulty is that the normalization coefficient $C(k)$ is not known analytically and so, in performing the integral over (k,y_1,y_2), it must be computed as a subsidiary integral. The other problem is the dependence of the shape of $p(A/B,y,k)$ on the exponent $s=\omega/2k$

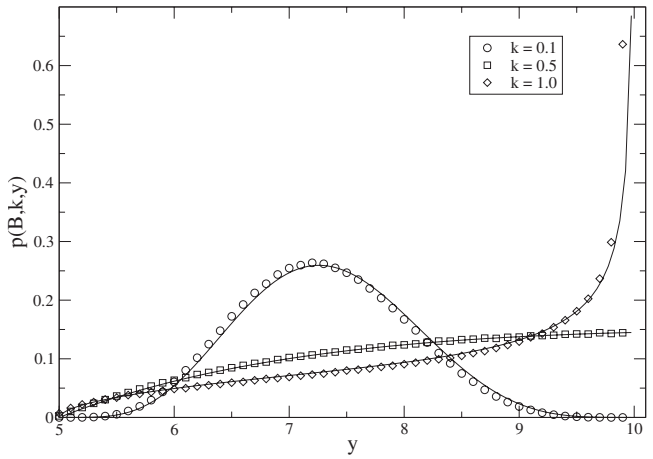

FIG. 3. Numerical and theoretical plots of the distribution $p(B,k,y)$ for the telegraph model defined in Sec. IV for $\epsilon_A=5.0$, $\epsilon_B=10.0$, $\omega=1.0$, and for $k=0.1,0.5,1.0$. The agreement is good and the minor discrepancy for $k=1.0$ is a symptom of the discrete nature of the numerical procedure. The value $k=0.5$ corresponds to the transition where $p(B,k,y)$ becomes nonzero at $y=\epsilon_B$. In general, for $k<1/2\omega$ we have $p(B,k,y=\epsilon_B)=0$ and for $k\geq 1/2\omega$ $p(B,k,y=\epsilon_B)>0$. This behavior has a strong effect on the Hamaker coefficient.

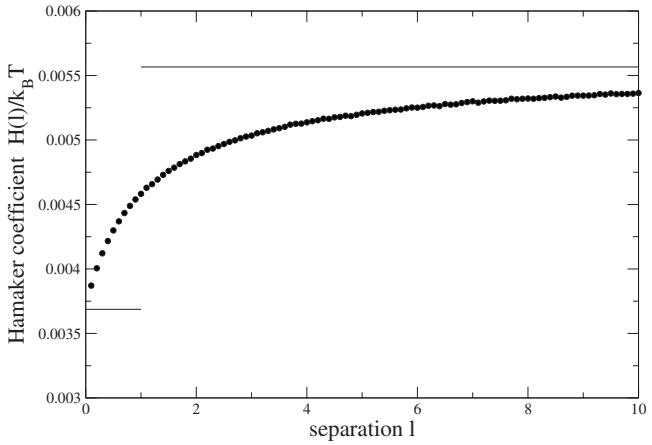

FIG. 4. The effective Hamaker coefficient $H(l)$ defined in Eq. (93) for the telegraph model defined in Sec. IV for $\epsilon_A=1.0$, $\epsilon_B=10.0$, $\omega=1.0$. The distribution function is $p(k,y)=p(A,k,y)+p(B,k,y)$ where $p(A/B,k,y)$ are given in Eqs. (81) and (82). Note that the curve is strongly dependent on separation l for $l\sim 1.0$ which corresponds to the transition in the behavior of $p(k,y)$ at $k=0.5\equiv 1/2\omega$. We would expect in the general case that this strong dependence occurs for $l\leq 1/2\omega$. The error bars on the points are within the symbol size. The asymptotic values for $l\to 0$ and $l\to\infty$ are also shown. In this case they are $H(l)/k_BT\to 3.688\ 10^{-3}\ l\to 0$, $H(l)/k_BT\to 5.666\ 10^{-3}\ l\to\infty$.

$$\left.\begin{aligned} p(A,y,k) &\propto \frac{1}{(y-\epsilon_A)^{1-s}} \\ p(B,y,k) &\propto \frac{1}{(\epsilon_B-y)^{1-s}} \end{aligned}\right\} \quad s\to 0,$$

$$p(A/B,y,k)\sim \delta(y-\epsilon^*) \quad s\to\infty, \tag{86}$$

where $\epsilon^*=\sqrt{\epsilon_A\epsilon_B}$. Depending on separation l the integral samples different regimes of k and hence of s, emphasizing $s\to 0(\infty)$ for $l\to 0(\infty)$. The probability distributions have completely different singular properties in these two limits and this causes difficulty with the numerical evaluation of the normalization $C(k)$ and of the three-dimensional integral itself. However, using adaptive Monte Carlo integration and a judicious choice of variable transformation, the value of $H(l)$ is accurately obtained for a wide range of values for l. Using Eq. (86) the small and large l limits for $H(l)$ can be obtained. For $l\to 0$, $H(l)$ tends to the average of the values for the four dielectric combinations $(\epsilon_1,\epsilon_2)=(\epsilon_A,\epsilon_A),(\epsilon_B,\epsilon_A),(\epsilon_A,\epsilon_B),(\epsilon_B,\epsilon_B)$; for $l\to\infty$, $H(l)$ tends to the value given by $\epsilon_1=\epsilon_2=\epsilon^*$. In these limits the values can be easily computed by other means. To illustrate the effects we chose $\epsilon_A=1$, $\epsilon_B=10$ which emphasizes the large variation between the small and large l values. The results are shown in Fig. 4 where the asymptotic values,

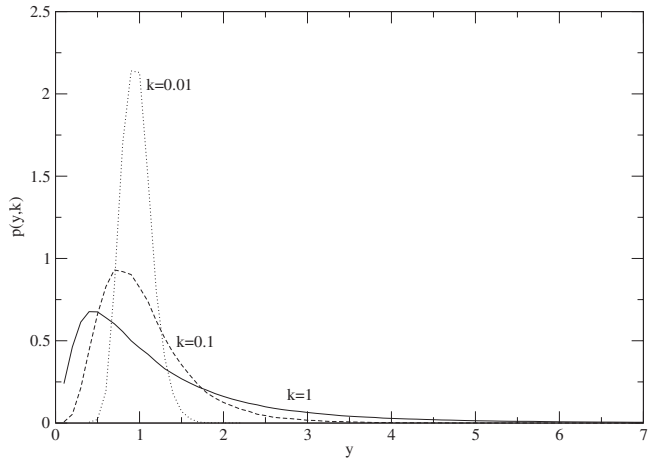

FIG. 5. Probability density for α for $k=1,0.1,0.01$ for $\epsilon(z)=\exp(\psi(z))$ where ψ is the OU Gaussian process with correlation function given by Eq. (69). The distribution $p(y,k)$ becomes sharply peaked around $y=1$ which is as predicted for small k, ϵ^* given by Eq. (31)

$$\frac{H(l)}{k_BT} \to 3.688 \times 10^{-3}\ l \to 0, \quad \frac{H(l)}{k_BT} \to 5.666 \times 10^{-3}\ l \to \infty, \tag{87}$$

are shown. As can be seen there is a strong variation in this model in the region around $l \sim 1$. Note that the length units are set by the ω parameter in the definition of the model; we chose $\omega=1$ here.

We next study the case where $\epsilon(z)$ is an instance drawn from the log-normal distribution give by Eq. (55). In the large slab separation (large l) the results are summarized by Eqs. (32) and (31), and in the small separation limit (small l) we expect Eq. (52) to hold; our simulations do indeed show that these equations are correct in the relevant limit.

A time-consuming part of the computation is the construction of an instance of the field $\epsilon(z)$ from the log-normal ensemble. We use the Fourier mode representation for an instance of the Gaussian field $\psi(z)$ which can be written as

$$\psi(z) = \frac{1}{N}\sum_{n=1}^{N} \cos(p_n z + \delta_n). \tag{88}$$

We chose the number of terms $N=64$. The phases δ_n are uncorrelated and chosen from a flat distribution $\delta_n \in (0,2\pi]$. The wave vectors p_n are also uncorrelated and chosen from the distribution $\tilde{G}(p)$ where the autocorrelation or two-point function of the ψ field is given by

$$\langle \psi(z)\psi(z')\rangle = \int \frac{dp}{2\pi}\tilde{G}(p)e^{ip(z-z')} \equiv G(z-z'). \tag{89}$$

A given choice for the set (p_n,δ_n), $n=1,\ldots,N$ determines a given instance of $\psi(z)$ and hence of $\epsilon(z)$. We took advantage of the scaling symmetry in Eq. (24) to reduce the amount of computation required. The simulations were done on 8–16 cores of a DELL T5400 with quadcore Xeon processors.

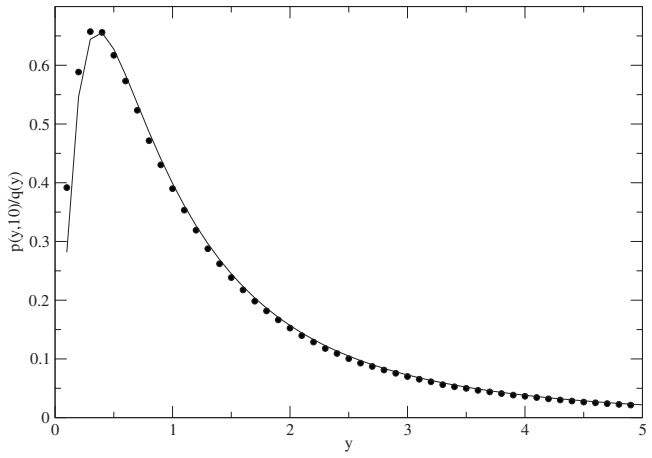

FIG. 6. The filled circles are the probability density for α for $k=10$ for $\epsilon(z)=\exp[\psi(z)]$ here ψ is the OU Gaussian process with correlation function given by Eq. (69) with $\omega=1$. The solid line is the probability density function $q(y)$ given in Eq. (90) for the same distribution of ϵ. The two distributions are already very close for $k=10$ in agreement with the prediction of Eq. (52).

We recall that for small k the values of α_1 and α_2 are predicted to be self-averaging and thus their distributions should be strongly peaked as $k \to 0$. In Fig. 5 we have simulated the system when ϵ is given by Eq. (55) and ψ is an OU Gaussian process [with $\lambda=1$ and $\epsilon_g=1$ in Eq. (55) and $\omega=1$ in Eq. (69)] for values of $k=1$ to 0.01. We see that as predicted the distribution of α becomes increasingly peaked about $\epsilon^*=1$ [as given by Eq. (31)] as the value of k is decreased. For large k the prediction Eq. (52) can be verified. Shown in Fig. 6 is the distribution for the same distribution of $\epsilon(z)$ but for $k=10$, we see that, as predicted, the probability density function for α is already very close to that of ϵ which is given by

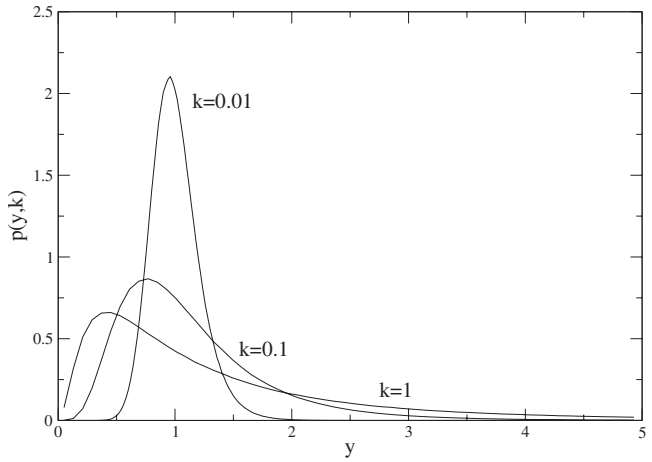

FIG. 7. Probability density for α for $k=1,0.1,0.01$ for $\epsilon(z)=\exp[\psi(z)]$ where ψ is the Gaussian process with correlation function given by Eq. (91). As for the OU process the distribution $p(y,k)$ becomes sharply peaked around $y=1$ which is as predicted for small k, and ϵ^* is given by Eq. (31)

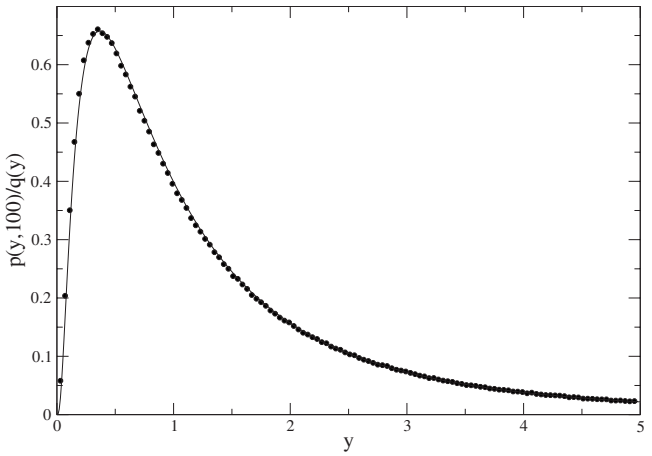

FIG. 8. The filled circles are the probability density for α for $k=100$ for $\epsilon(z)=\exp[\psi(z)]$ here ψ is the Gaussian process with correlation function given by Eq. (91) with $\omega=1$. The solid line is the probability density function $q(y)$ given in Eq. (90) for the same distribution of ϵ. The two distributions are already very close for $k=10$ in agreement with the prediction of Eq. (52).

$$q(y) = \frac{1}{\sqrt{2\pi y}} \exp\left(-\frac{1}{2}\ln^2(y)\right). \tag{90}$$

Note that $q(y)$ is independent of the correlation function of the Gaussian field in the log-normal distribution.

One can also consider the case of non-Markovian log-normal dielectric constants. For instance, one can take the field ψ in Eq. (55) to have correlation function

$$\langle \psi(z)\psi(z')\rangle = \exp[-\omega^2(z-z')^2/2]. \tag{91}$$

In what follows we fix $\lambda=1$ and $\omega=1$. For the small values of k shown in Fig. 7 we see again that as $k\to 0$ that the distribution becomes peaked about $\epsilon^*=1$ as predicted. In Fig. 8, we show the comparison between the distribution of α and ϵ, again at this value of k the agreement between the two distributions is already excellent.

We also compute the average effective Hamaker coefficient as a function of separation l using Eq. (23) to define

$$\langle H(l)\rangle = \frac{k_B T}{16\pi}\int udu \int dy_1 dy_2 p_1(u/2l,y_1)p_2(u/2l,y_2) \times \ln(1-\Delta(y_1)\Delta(y_2)\exp(-u)), \tag{92}$$

with $\Delta(y)=(y-\epsilon_0)/(y+\epsilon_0)$. For $\epsilon(z)$ distributed according to the log-normal distribution in Eq. (55) and using the scaling result in Eq. (24) we can write

$$\langle H(l;\epsilon_g)\rangle = \frac{k_B T}{16\pi}\int udu \int dy_1 dy_2 p_1(u/2l,y_1)p_2(u/2l,y_2) \times \ln[1-\Delta(\epsilon_g y_1)\Delta(\epsilon_g y_2)\exp(-u)], \tag{93}$$

where the $p_i(k,y)$ are computed for $\epsilon_g=1$. The computation is very time consuming since for each value of l a three-dimensional integral must be performed over (k,y_1,y_2), and for each value of k the probability distribution must be constructed, as described earlier, by integrating Eq. (26) over many realizations of the log-normal field $\epsilon(z)$. It might be thought that it would be possible to compute $p(k,y)$ once and for all and store the result for later use. However, this turns out to need a very large computer memory (RAM) size which is prohibitive.

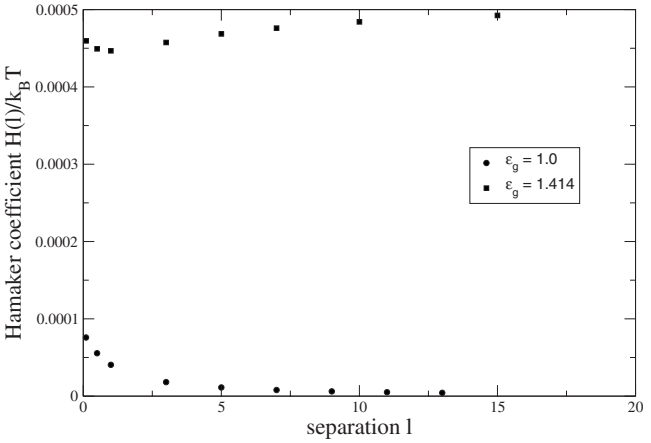

FIG. 9. The effective Hamaker coefficient $H(l)$ defined in Eq. (93) for the distribution defined by Eqs. (55) and (91) for $\epsilon_g=1.0, 1.414$. In both cases the curves are asymptotic to the Hamaker constant for a homogeneous system with dielectric constant $\epsilon^*=\sqrt{\langle\epsilon\rangle/\langle 1/\epsilon\rangle}$. Notably, $\epsilon^*=1$ for $\epsilon_g=1.0$ and we see that $H(l)$ is asymptotic to zero from above showing that the force is attractive for all l even in this case. As is also seen, the curves are asymptotic either above or below depending on the value of ϵ_g and is not necessarily monotonic.

We show $H(l;\epsilon_g)$ versus l in Figs. 9 and 10 for various values of ϵ_g. As can be seen $H(l)$ is asymptotic to the Hamaker constant for a homogeneous system with dielectric constant $\epsilon^*=\sqrt{\langle\epsilon\rangle/\langle 1/\epsilon\rangle}$, and that for $\epsilon_g=1.0$ that $H(l)$ is asymptotic to zero from above showing that the force is attractive for all l. This need not have been the case since there will be contributions from configurations were the dielectric constants ϵ_1,ϵ_2 in the slabs satisfy $\epsilon_1>1>\epsilon_2$ or vice versa;

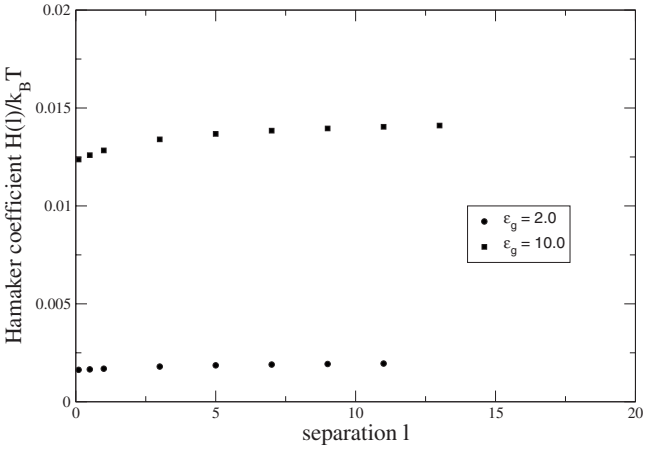

FIG. 10. The effective Hamaker coefficient $\langle H(l)\rangle$ defined in Eq. (93) for the distribution defined by Eqs. (55) and (91) for $\epsilon_g=2.0$, 10.0. In both cases the curves are asymptotic to the Hamaker constant for a homogeneous system with dielectric constant $\epsilon^*=\sqrt{\langle\epsilon\rangle/\langle 1/\epsilon\rangle}$.

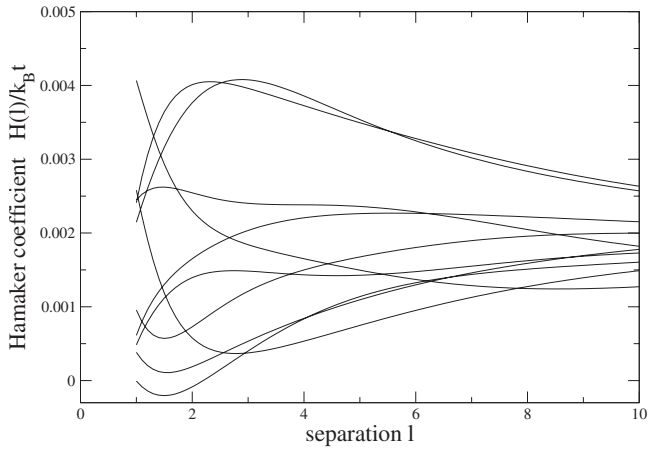

FIG. 11. Examples of the Hamaker coefficient from the ensemble generated by the distribution for $\epsilon(z)$ for $\epsilon_g=2.0$ plotted versus separation l. The average curve of the ensemble is shown in Fig. 10. Note that for small l the curvature of the ensemble curves are not of definite sign

such configurations contribute a repulsive contribution to the force. As is also observed, the curves are either asymptotic from above or below and are not necessarily monotonic but can have an initial decrease before rising to the asymptotic value. These are significant features due to the random nature of the system.

In Figs. 11 and 12 we show a sample of the Hamaker coefficients for particular realizations of $\epsilon(z)$ plotted against separation l and for $\epsilon_g=2.0, 10.0$, respectively. The averages over the ensembles from which these curves are taken are given in Fig. 10. It is important to note that the curvatures of the ensemble curves are not of definite sign and that for small l there are both curves that decrease and curves that increase with l. These properties are reflected in the shape of the curve for the ensemble average.

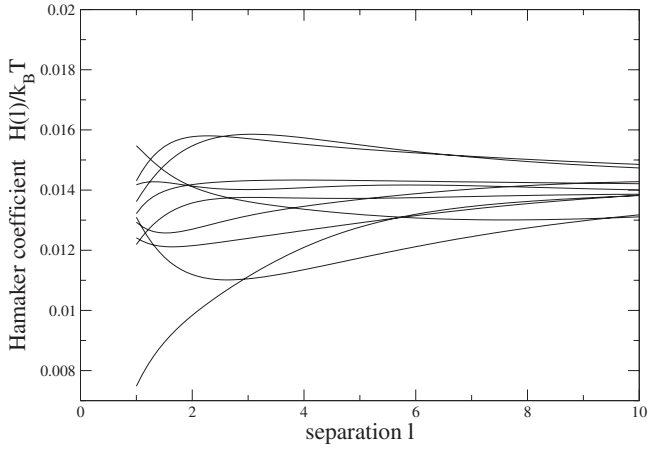

FIG. 12. Examples of the Hamaker coefficient from the ensemble generated by the distribution for $\epsilon(z)$ for $\epsilon_g=10.0$ plotted versus separation l. The average curve of the ensemble is shown in Fig. 10. Note that the curvatures of the ensemble curves are not of definite sign.

VI. CONCLUSIONS

We have obtained the limiting behavior of the thermal Casimir effect in the limit of large separation between the slabs, where the free energy is given by self-averaging and thus the distributions of $\alpha(k,z)$ are strongly peaked. We have shown that the interaction between two homogeneous media is stronger than that between the two fluctuating media if $\langle 1/\epsilon\rangle^{-1} > \epsilon_0$. However it is always weaker if $\langle \epsilon\rangle < \epsilon_0$. We thus see that, depending on the details of the distribution of the fluctuating dielectric response in the two slabs and the dielectric response of the medium in between, the effective interaction at large inter-slab separations can be stronger or weaker than that for a uniform medium with a dielectric function equal to the average value of that of the media in which it fluctuates. In the limit of small separation, where the interaction free energy is a random variable that has to be averaged over the probability density function of the dielectric functions in the media composing the two interacting slabs.

The intermediate length scales were analyzed via perturbation theory and models of disorder that can be treated numerically. All numerical simulations completely corroborate the analytical results for self-averaging at large separations.

We carried out numerical studies of two models characterized by very different random distributions of dielectric constant. The telegraph model is described in Sec. IV and analytic solutions are given for the marginal probability distributions for the effective dielectric variable y, $p(A/B,k,y)$, where A/B label the two choices of slab dielectric constant $\epsilon_{A/B}$ and k is the modulus of the wave-vector for the transverse mode; the distribution relevant to the computation of the Hamaker coefficient $H(l)$ is $p(k,y)=p(A,k,y)+p(B,k,y)$. The frequency with which the dielectric constant switches between $\epsilon_{A/B}$ as a function of z is controlled by the parameter ω. We find a sharp transition in the shape of $p(k,y)$ depending on whether $k<\omega/2$ ior $k>1/2/\omega$ and this has a strong effect on $H(l)$ which varies strongly for $l \leq 1/2\omega$. These effects are clearly shown in Figs. 2–4.

The model where $\epsilon(z)$ is given by a log-normal distribution Eq. (55) with auto-correlation function given in Eq. (91) requires a numerical solution for $p(k,y)$ each value of k in the integral expression for $H(l)$ in Eq. (92). This is computationally very time-consuming but is tractable. The resulting distributions agree with the predicted shapes for large k as is seen in Fig. 6. The behavior of $H(l)$ for various choices of ϵ_g are plotted and $H(l)$ is shown to have a nonmonotonic behavior for intermediate values of ϵ_g.

The nonlinear formulation of the problem presented here should be equally useful to treat the case of deterministically varying dielectric functions and could open up a useful computational framework for designing materials where the effective interaction can be tuned, to induce attractive or repulsive forces depending on the separation [16]. The formulation also means that if one knows the coefficients $a_i(k)$, $a_f(k)$ and $b_j(k)$ for any set of slab media, then one can immediately compute the effective interaction between them at any distance. This is a rather surprising result as if one wanted to compute the effective interaction between two media (1) and (2) using the pair wise approximation, $1/r^6$ for

the van der Waals interaction, it is clear that medium (1) needs to know what is in medium (2) at each point in order to compute the force. The decomposition in terms of Fourier modes however means that the interaction between the two media is effectively factorized. A number of further applications of our method would be to examine the role of disorder for the nonzero frequencies corresponding to quantum fluctuations and also for different geometries, such as cylindrical and spherical, when the dielectric function varies only in the radial direction. An interesting open problem concerns what happens when the dielectric function varies in all directions, it would be interesting to know if one can prove in this case whether the long-distance interaction between two slabs is also given by the same effective medium expression as derived here.

ACKNOWLEDGMENTS

This research was supported in part by the National Science Foundation under Grant No. PHY05-51164 (while at the KITP program *The theory and practice of fluctuation induced interactions*). D.S.D. acknowledges support from the Institut Universitaire de France. R.P. would like to acknowledge the financial support by the Agency for Research and Development of Slovenia, Grants No. P1-0055C, No. Z1-7171, and No. L2-7080. This study was supported in part by the Intramural Research Program of the NIH, Eunice Kennedy Shriver National Institute of Child Health and Human Development. A.N. thanks the Royal Society, the Royal Academy of Engineering, and the British Academy (UK).

[1] M. Bordag, G. L. Klimchitskaya, U. Mohideen, and V. M. Mostepanenko, *Advances in the Casimir Effect* (Oxford University Press, New York, 2009).
[2] E. J. W. Verwey and J. Th. G. Overbeek, *Theory of the Stability of Lyophobic Colloids* (Elsevier, Amsterdam, 1948); J. N. Israelachvili, *Intermolecular and Surface Forces* (Academic Press, London, 1990).
[3] J. Mahanty and B. W. Ninham, *Dispersion Forces* (Academic Press, London, 1976).
[4] V. A. Parsegian, *Van der Waals Forces* (Cambridge University, Cambridge, 2006).
[5] I. E. Dzyaloshinskii, E. M. Lifshitz, and L. P. Pitaevskii, Adv. Phys. **10**, 165 (1961).
[6] H. B. G. Casimir, Proc. K. Ned. Akad. Wet. **51**, 793 (1948).
[7] D. S. Dean, R. R. Horgan, A. Naji, and R. Podgornik, Phys. Rev. A **79**, 040101(R) (2009).
[8] A. Naji, D. S. Dean, J. Sarabadani, R. R. Horgan, and R. Podgornik, Phys. Rev. Lett. **104**, 060601 (2010).
[9] R. Podgornik and V. A. Parsegian, J. Chem. Phys. **121**, 7467 (2004).
[10] D. S. Dean and R. R. Horgan, Phys. Rev. E **65**, 061603 (2002); **71**, 041907 (2005); **76**, 041102 (2007); J. Phys. C **17**, 3473 (2005).
[11] C. Itzykson and J.-M. Drouffe, *Statistical Field Theory: Strong Coupling, Monte Carlo Methods, Conformal Field Theory and Random Systems* (Cambridge University Press, Cambridge, 1991), Vol. 2.
[12] G. Veble and R. Podgornik, Phys. Rev. B **75**, 155102 (2007).
[13] R. Podgornik and V. A. Parsegian, J. Chem. Phys. **120**, 3401 (2004).
[14] D. S. Dean, R. R. Horgan, and I. T. Drummond, J. Stat. Mech.: Theory Exp. (2007), P07013.
[15] H. Risken, *The Fokker-Planck Equation*, 3rd ed. (Springer-Verlag, New York, 1996).
[16] J. Bárcenas, L. Reyes, and R. Esquivel-Sirvent, Appl. Phys. Lett. **87**, 263106 (2005); J. N. Munday, F. Capasso, and V. A. Parsegian, Nature (London) **457**, 170 (2009).